Preparation, characterization and Cr(VI) adsorption evaluation of NaOH-activated carbon produced from Date Press Cake; an agro-industrial waste

Samira Norouzi[a], Mohsen Heidari[a,*], Vali Alipour[a], Omid Rahmanian[a], Mehdi Fazlzadeh[b,c], Fazel Mohammadi-moghadam[d], Heshmatollah Nourmoradi[e,f], Babak Goudarzi[a], Kavoos Dindarloo[a]

[a] Department of Environmental Health Engineering, Faculty of Health, Hormozgan University of Medical Sciences, Bandar Abbas, Iran
[b] Social Determinants of Health Research Center, Department of Environmental Health Engineering, School of Health, Ardabil University of Medical Sciences, Ardabil, Iran
[c] Department of Environmental Health Engineering, School of Public Health, Tehran University of Medical Sciences, Tehran, Iran
[d] Department of Environmental Health Engineering, Faculty of Health, Shahrekord University of Medical Sciences, Shahrekord, Iran
[e] Department of Environmental Health Engineering, Faculty of Health, Ilam University of Medical Sciences, Ilam, Iran
[f] Biotechnology and Medical Plants Research Center, Ilam University of Medical Sciences, Ilam, Iran

ARTICLE INFO

ABSTRACT

Date Press Cake (DPC) is an inevitable by-product of date processing industries and may pose environmental problems if not managed properly. In this study, DPC was converted into activated carbon using solid NaOH under various activation conditions. The prepared activated carbon showed high specific surface area ($2025.9 \, \mathrm{m^2 \, g^{-1}}$) and microporous texture (86.01%). It was successfully applied for the adsorption of Cr(VI) from aqueous solutions with maximum monolayer adsorption capacities as high as $282.8 \, \mathrm{mg \, g^{-1}}$ (pH = 2) and $198.0 \, \mathrm{mg \, g^{-1}}$ (pH = 5). The kinetic and isotherm experimental data of Cr(VI) adsorption onto the activated carbon were best described by Elovich and Redlich-Peterson models, respectively. It was found that the Cr(VI) adsorption onto the DPC-derived activated carbon was predominantly a chemisorption process with limited desorption rates (below 50%). Overall, Date Press Cake could be considered as an abundant and renewable agro-industrial precursor for the production of high quality activated carbon.

1. Introduction

Chromium is a top-priority heavy metal and its occurrence in water bodies is a paradigm of industrial pollution (Fazlzadeh et al., 2017). Chromium is introduced into the aquatic environments from a variety of industrial processes such as petroleum refining, metallurgy, tanning, electroplating, battery, textile and dye manufacturing (Yang et al., 2015). This compound exists in aquatic ecosystems as hexavalent, Cr (VI), and trivalent, Cr(III), forms. Cr(III) is basically immobile in aqueous environment due to its very low water solubility, especially at neutral and basic conditions. In the other hand, Cr(VI) is highly water soluble, $\sim 10^5 \, \mathrm{mg \, L^{-1}}$, and can be transported great distances before being reduced to Cr(III) (Pawlisz et al., 1997). Cr(III) is a human micronutrient, while Cr(VI) is toxic and can cause severe diseases such as kidney circulation, dermatitis and lung cancer (Owlad et al., 2009). Therefore, removing this pollutant from aquatic environments is essential for the protection of environment and public health.

The commonly used methods for the removal of Cr(VI) from aqueous environments are reduction, membrane filtration, precipitation, and ion exchange (Pehlivan et al., 2008; Fazlzadeh et al., 2017). These methods have many disadvantages including high energy consumption, large quantities of input chemicals, high capital and operational cost, production of large amounts of sludge and possible generation of secondary pollution (Owlad et al., 2009; Gupta et al., 2011; Al-Othman et al., 2012). In the other hand, adsorption process has gained increasing attention due to its simplicity of design and operation, high efficiency, low treatment cost and possible recovery of the pollutant (Wang et al., 2010; Gupta and Saleh, 2013; Kumar and Jena, 2017b). For these reasons, more focus has been directed toward the research on the development and optimization of novel and effective adsorbents in recent years. In this regard, various natural and synthetic materials, whether organic or inorganic, have been applied for Cr(VI) adsorption from aqueous solutions.

Activated carbon is a well-known adsorbent due to its extended surface area, high adsorption capacity, fast kinetics and relatively easy regeneration (Sathishkumar et al., 2012). However, large-scale usage of

---

this adsorbent is hampered when it produced from expensive and non-renewable precursors (Ahmaruzzaman and Gupta, 2011; Cazetta et al., 2011). Therefore, it is necessary to research and develop activated carbons from low cost and abundant precursors. Several literatures has focused on Cr(VI) removal from aqueous solutions using activated carbons prepared from a variety of agricultural wastes including Tobacco residues (Kilic et al., 2011), Longan seed (Yang et al., 2015), Aegle Marmelos fruit shell (Gottipati and Mishra, 2016), Mango kernel (Rai et al., 2016) and Fox nutshell (Kumar and Jena, 2017a).

In date processing industries, date juice is separated from fibrous material using filter press. Thus, the remained fibrous material, here named Date Press Cake (DPC), is an inevitable by-product of such industries (Chandrasekaran and Bahkali, 2013; Ghnimi et al., 2017). According to the Food and Agriculture Organization of the United Nations (FAO), the amount of date fruit produced in Iran was 1,156,996 tons in 2014 (FAO, 2014). In Hormozgan province (one of the country's largest date fruit producers), a huge amount of DPC is produced daily and mainly dumped into open lands and drains. The dumped DPC, which may pose environmental problems, can be considered as an abundant, cheap and renewable precursor for the production of activated carbon.

To the best of our knowledge, no work has been found in literature on the production of activated carbon from Date Press Cake through chemical activation. Therefore, this environmentally problematic waste was considered as a new precursor for the production of activated carbon, which may be useful for the purification of polluted aquatic environments. In this regard, the main aims of this study were to prepare activated carbon from DPC and to evaluate its application for the adsorption of Cr(VI) from aqueous solutions. The main textural and surface properties of the prepared activated carbon were evaluated, before and after Cr(VI) adsorption. The adsorption kinetic and isotherm studies as well as desorption studies were also conducted.

2. Materials and methods

2.1. Chemicals and materials

Sodium hydroxide ($\geq 99.0\%$ purity), hydrochloric acid (37% purity), potassium dichromate ($\geq 99.9\%$ purity), sodium hydrogen carbonate ($\geq 99.0\%$ purity), sodium bicarbonate ($\geq 98.0\%$ purity), and the chemicals used for the determination of the different states of chromium (sulfuric acid (98% purity), 1,5-diphenylcarbazide ($\geq 98.0\%$ purity), potassium permanganate ($\geq 99.0\%$ purity), ammonia (32% purity) and acetone ($\geq 99.8\%$ purity)) were purchased from Merck Co., Germany. Stock solution of $1000\,mg\,L^{-1}$ Cr(VI) was prepared by dissolving a given amount of potassium dichromate in deionized water and the required standard solutions were obtained from the stock solution. Raw Date Press Cake was kindly obtained from a local date processing industry and dried at 105 °C.

2.2. Preparation of activated carbon

Due to unstable structure of raw DPC, like that of biological sludge, an amount of this material (mainly soluble fraction) may be lost during initial washing and direct impregnation with chemical activating agents. In this regard, activated carbon was prepared through a two-step procedure according to the methods proposed by Cazetta et al (2011) and Pezoti et al (2016) with some modifications, i.e. initial carbonization and chemical activation with NaOH pellets under dry conditions. First, the dried DPC, with particle size below 1 mm, was put into a stainless steel reactor and heated at a rate of $20\,°C\,min^{-1}$ to 500 °C. After 2 hr heating, the obtained carbonized material (CM) allowed to be gradually cooled. Second, CM was further ground to particle size below $500\,\mu m$ and physically mixed with NaOH pellets at weight ratio of 2:1 (NaOH:CM). The mixture was put into a stainless steel reactor and heated under nitrogen flow of $100\,ml\,min^{-1}$ at a rate

of $20\,°C\,min^{-1}$ to the various final temperatures (450–750 °C) and maintained for 90 min at these conditions. Thereafter, the mixture was cooled under nitrogen flow and the obtained material was washed on a filter with deionized water and dilute HCl, repeatedly, until the pH of filtrate became neutral. The obtained material, activated carbon (AC), was dried at 105 °C overnight. Based on Cr(VI) adsorption capacity of the prepared ACs, the optimum temperature for the preparation of AC was selected. The selected temperature was applied for AC preparation at various levels of NaOH:CM weight ratio (1:1–4:1). The prepared activated carbons were labeled as AC-x-y, where AC represents activated carbon, x donates activation temperature and y stands for weight ratio of NaOH to CM. The yield values based on the original weight of the raw material were determined as follow:

$$Yield\,(\%) = \frac{W_C}{W_R} \times 100 \tag{1}$$

where W_C and W_R are the dry weights of CM or ACs and raw material (g), respectively.

2.3. Adsorption experiments

The experiments for the adsorption of Cr(VI) onto prepared AC from DPC were done in batch mode by taking 25 ml of Cr(VI) solution into 50 ml Erlenmeyer flasks. The experiments for the selection of best conditions for AC preparation were done at the following conditions; initial Cr(VI) concentration of $100\,mg\,L^{-1}$, contact time of 180 min and natural solution pH (≈ 5).

After selecting the best conditions for AC preparation, the effect of solution pH (1–9) on Cr(VI) adsorption was evaluated with initial Cr(VI) concentration of $300\,mg\,L^{-1}$ at 180 min contact time. The kinetics of Cr(VI) adsorption on the selected AC was done at contact times ranged from 2.5 to 360 min with initial Cr(VI) concentration of $300\,mg\,L^{-1}$ and two different pH values. Isotherm analysis was performed at the following conditions; initial Cr(VI) concentrations ranged from 5 to $450\,mg\,L^{-1}$, equilibrium contact time and two different pH values.

The effect of ionic strength on Cr(VI) adsorption was tested with i) deionized water containing various molar NaCl concentrations and ii) real seawater with various ionic strength levels through diluting it with deionized water. Seawater was considered as a very strong natural ionic solution (EC = $72,750\,\mu S\,m^{-1}$) containing a complex mixture of natural salts. All the tests were done in $300\,mg\,L^{-1}$ Cr(VI) solutions at equilibrium contact time.

In all adsorption tests, the adsorbent dose was $1\,g\,L^{-1}$. Before adsorbent addition, the initial pH of the Cr(VI) containing solutions was adjusted by dilute HCl or NaOH. A calibrated pH meter was used for the measurement of pH (WTW, Germany). At the end of each adsorption experiment, the adsorbent was separated from suspension using membrane filter. The concentrations of Cr(VI) and Cr(III) in the filtrate were determined according to the colorimetric method proposed by the standard methods for the examination of water and wastewater (3500-Cr). Cr(VI) was determined colorimetrically by reaction with diphenylcarbazide in acidified solution. The developed red-violet color was measured using a double beam spectrophotometer (SP-1900 UV–vis) at 540 nm wavelength. In order to determine the Cr(III) concentration, all chromium content of the samples was converted to the hexavalent state by oxidation with potassium permanganate. The process for the determination of Cr(VI) was again performed. Finally, the concentration of Cr(III) was estimated as the difference between the concentrations of Cr(VI), after and before oxidation step (Federation, 2005).

The adsorption capacity (q_e and q_t) and removal efficiency (RE) of Cr(VI) by AC were calculated as follows:

$$q_e = \frac{(C_i - C_e)V}{W} \tag{2}$$

$$q_t = \frac{(C_i - C_t)V}{W} \qquad (3)$$

$$RE = \frac{(C_i - C_t)}{C_i} \times 100 \qquad (4)$$

where C_i, C_e and C_t are the initial, equilibrium and at time t of Cr(VI) concentrations ($mg\,L^{-1}$), respectively, V is the volume of suspension (L), and W is the dry weight of the adsorbent in suspension (g).

2.4. Desorption experiments

The desorption of Cr(VI) from loaded activated carbon was carried out with various eluents including HCl, H_3PO_4, HNO_3, NaOH and KOH. Initially, the adsorbent was loaded with Cr(VI) at the following conditions: initial Cr(VI) concentration $300\,mg\,L^{-1}$, pH 2, adsorbent dose $1\,g\,L^{-1}$ and equilibrium contact time. After adsorption, the suspension was filtered and the Cr(VI) loaded adsorbent was placed in the desorbing solutions and stirred. After a given contact time, the adsorbent was separated and the amount of desorbed Cr(VI) was measured via above-mentioned procedure. The desorption rate of Cr(VI) was calculated as:

$$Desorption\ rate\ (\%) = \frac{amount\ of\ Cr(VI)\ desorbed}{amount\ of\ Cr(VI)\ adsorbed} \times 100$$

All the batch experiments were duplicated under the same conditions and the mean values are reported. Note that all adsorption and desorption experiments were done at stirring rate and temperature of 250 rpm and 298 ± 0.5 K, respectively.

2.5. Adsorbent characterization

Textural properties of selected AC were characterized by N_2 adsorption-desorption at 77 K using a surface area analyzer (Belsorp-mini II, BEL Japan Inc., Osaka, Japan). Brunauer–Emmett–Teller (BET) isotherm was applied for the estimation of specific surface area or S_{BET}. Total pore volume, V_T, of selected AC was determined based on the amount of nitrogen adsorbed onto the material surface at relative pressure (P/P^0) of 0.99 (Basta et al., 2009). Micropore volume was determined based on the volume of adsorbed N_2 at P/P^0 of 0.1, and mesopore volume was calculated by subtracting the amount of adsorbed N_2 at P/P^0 of 0.1 from that at 0.95 (Horikawa et al., 2008). Pore size distribution was ascertained using the method of Barrett-Joyner-Halenda (BJH) and average pore diameter, D_p, was calculated using the relation $4V_T/S_{BET}$ (Cazetta et al., 2011). The morphology and elemental composition of selected AC, before and after Cr(VI) adsorption, were analyzed by a field emission scanning electron microscope coupled with a dispersive X-ray spectrometer (FESEM-EDX, Tescan Mira 3 LMU). The X-ray diffraction (XRD) of the adsorbent, before and after Cr(VI) adsorption, was performed using Philips X'Pert X ray diffractometer (model PW 1730) with Cu Kα radiation within 2θ range of 10–80°.

Fourier transform infrared (FT-IR) spectroscopy (Nicolet Avatar 360, Nicolet, USA) was used for the analysis of the functional groups present on the surface of selected AC, before and after Cr(VI) adsorption. The FT-IR spectra were recorded over the wavenumber range of 4000–400 cm^{-1} at 4 cm^{-1} resolution and 20 scans min^{-1}.

Additionally, the chemical characteristics of selected AC were analyzed by Boehm titration according to the method proposed by Goertzen et al. (2010). The acid and base functional groups were determined through neutralization of them with NaOH (carboxylic, lactonic and phenolic acids), Na_2CO_3 (carboxylic and lactonic acids), $NaHCO_3$ (carboxylic acid) and HCl (basic groups). The point of zero charge pH (pH_{PZC}) was determined using pH drift procedure (Liu et al., 2011).

Table 1
General forms of the kinetic and isotherm models used in this study.

Kinetic models	
Pseudo-first order	$q_t = q_e(1 - e^{-k_1 t}); h_0 = k_1 q_e$
Pseudo-second order	$q_t = \frac{k_2 q_e^2 t}{1 + k_2 q_e t}; h_0 = k_2 q_e^2$
Elovich	$q_t = \frac{1}{\beta}\ln(1 + \alpha\beta t)$
Intraparticle Diffusion	$q_t = k_{id}\sqrt{t} C_i$
Boyd	$B_t = -\ln\left(1 - \frac{q_t}{q_e}\right) - 0.4977$
Isotherm models	
Freundlich	$q_e = k_F C_e^{1/n_f}$
Langmuir	$q_e = \frac{q_m k_L C_e}{1 + k_L C_e}; R_L = \frac{1}{1 + k_L C_0}$
Redlich-Peterson	$q_e = \frac{a_{RP} C_e}{1 + b_{RP} C_e^g}$
Temkin	$q_e = \frac{RT}{b_T}\ln(k_T C_e)$

k_1 and k_2 = rate constants of the pseudo-first order and pseudo-second order models, respectively; h_0 = initial adsorption rate; α and β = Elovich constants; k_{id} and C_i = intraparticle diffusion constants; B_t = Boyd constant; k_F and n_f = Freundlich constants; q_m = maximum monolayer adsorption capacity; k_L = Langmuir constant; R_L = Langmuir separation factor; a_{RP}, b_{RP} and g = Redlich-Peterson constants; b_T = variation of the adsorption energy in Temkin model; k_T = Temkin constant; R = universal gas constant ($8.314\,j\,mol^{-1}\,K^{-1}$); T = absolute temperature (K).

2.6. Data analysis

In order to understand the dynamics of Cr(VI) adsorption, the experimental q_t data at various contact times were fitted with some kinetic models including Pseudo-first order, Pseudo-second order, Elovich, Intraparticle diffusion, and Boyd. Moreover, four common isotherm models, namely Freundlich, Langmuir, Redlich-Peterson and Temkin, were applied for the analysis of the equilibrium experimental data.

The general forms of the kinetic and isotherm models used in this study are listed in Table 1 (Martins et al., 2015; Pezoti et al., 2016). The experimental adsorption data were fitted by the linearized Intraparticle diffusion and Boyd kinetic models. In the other hand, the non-linear forms of other kinetic models and all the isotherm models were fitted to the experimental adsorption data using OriginLab Pro (2018) software.

The best-fitted kinetic and isotherm models were identified by the coefficient of determination (R^2) and the residual root-mean squared error (RMSE). Their equations are given as follows;

$$R^2 = 1 - \frac{\sum_{n=1}^{n}(q_{exp} - q_{cal})^2}{\sum_{n=1}^{n}(q_{cal} - \overline{q_{cal}})^2} \qquad (5)$$

$$RMSE = \sqrt{\frac{1}{n-1}\sum_{n=1}^{n}(q_{exp} - q_{cal})^2} \qquad (6)$$

where q_{exp} ($mg\,g^{-1}$) and q_{cal} ($mg\,g^{-1}$) are the experimental- and calculated Cr(VI) adsorption capacities, respectively, at equilibrium (isotherm) and time t (kinetic), and n is the number of data points. Higher R^2 and lower RMSE values indicate more accurate fitting of the models.

3. Results and discussion

3.1. Selection of best activation conditions

In order to find the best conditions for AC preparation, various levels of NaOH:CM ratio and activation temperature were applied in activation process. The Cr(VI) adsorption capability of the produced ACs at each activation condition was used as activation performance index. Fig. 1 shows the effects of activation temperature and NaOH:CM ratio on the Cr(VI) adsorption rate of the produced carbon. It is evident
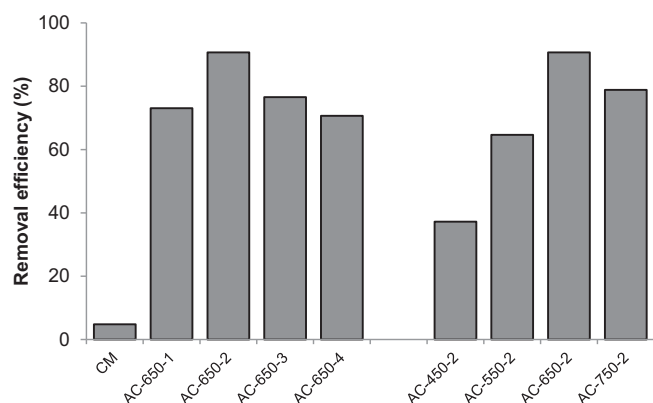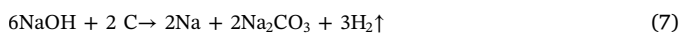
Fig. 1. Effects of NaOH:CM weight ratio and activation temperature on the Cr(VI) adsorption capacity of prepared activated carbons.

that NaOH activation led to a dramatic increase in Cr(VI) adsorption rate as compared to the original CM, indicating the positive effect of NaOH activation process on CM structure. The NaOH activation process is presumed to involve redox reduction and carbon oxidation (Xia et al., 2016). Some possible reactions may occur between carbon surface and active intermediates according to the following equations:

$$6NaOH + 2\,C \rightarrow 2Na + 2Na_2CO_3 + 3H_2\uparrow \tag{7}$$

$$Na_2CO_3 \rightarrow Na_2O + CO_2\uparrow \tag{8}$$

$$2Na + CO_2 \rightarrow Na_2O + CO\uparrow \tag{9}$$

The redox reactions along with the release of the gaseous products may generate porosity and then may increase adsorption sites on adsorbent surface. Moreover, the intercalation of the produced alkaline metal into the carbon structure could stabilize and widen the spaces between atomic layers of carbon (Foo and Hameed, 2012).

With increasing the activation temperature from 450 to 650 °C, the Cr(VI) adsorption capacities of the produced ACs were increased. In fact, the diffusion of NaOH molecules into the structure of CM and then the development of porosity may be facilitated at higher reaction temperatures (Tongpoothorn et al., 2011).

The AC prepared at 650 °C attained the highest potential for Cr(VI) adsorption. Further increase in activation temperature led to the reduced Cr(VI) adsorption potential of the produced AC. Therefore, the activation temperature of 650 °C was chosen for the preparation of activated carbon at various NaOH:CM ratios. As can be seen from Fig. 1, NaOH:CM ratio of 2:1 seems to be sufficient for AC preparation at 650 °C, since AC-650-2 showed the highest Cr(VI) adsorption capability. Further increases in NaOH:CM ratio and activation temperature reduced the Cr(VI) adsorption potential of the produced AC. Exorbitant activation conditions in activation process may expand the micropore to mesopore or macropore and then reduces the sorbent surface area for the adsorption of the pollutant (Adinata et al., 2007).

The above results imply that the best quality DPC-derived activated carbon in terms of Cr(VI) adsorption could be produced at NaOH:CM weight ratio and activation temperature of 2 and 650 °C, respectively. Therefore, AC-650–2 was selected for further Cr(VI) adsorption experiments.

3.2. Yield

The yield value based on the original weight of the raw material was of 45.5% for CM. After activation, the yield value almost halved. The loss in activated carbon weight could be related to the action of the activating agent at high temperature. The reaction between NaOH and carbon at high temperature provides elimination and dehydration reactions, which may break the bonds C–C and C–O–C of the organic material (Cazetta et al., 2011). The yield value of the selected

adsorbent, AC-650-2, was 26.2%, which is reasonable compared to those reported for some NaOH-activated carbons derived from agro-industrial wastes (Cazetta et al., 2011; Martins et al., 2015; Pezoti et al., 2016).

3.3. Textural characterization of the material

The N_2 adsorption-desorption isotherms and the pore size distribution of AC-650-2 are shown in Supplementary Material. According to IUPAC classification, the obtained adsorption isotherm profile could be classified as type I, which is typical of a microporous material (Silva et al., 2017).

The pore size distribution of AC-650-2 is displayed in Supplementary Material. Accordingly, the size of most pores was smaller than 2 nm with an average pore diameter of 1.839 nm, indicating the development of microporosity in adsorbent structure. The micropore and mesopore volumes were 0.801 and 0.099 $cm^3\,g^{-1}$, respectively, which correspond to 86.01% and 10.62% of total pore volume (0.932 $cm^3\,g^{-1}$). The simultaneous presence of micropores and mesopores in AC-650-2 may be beneficial for its adsorption capacity. It has been well known that the micropores provide a large number of adsorption sites, while mesopores facilitate the transfer of heavy metal ions (e.g., Cr, Cd, Pb, etc.) (Sun et al., 2017). BET surface area is one of the most important characteristics of adsorbent material, because more adsorption sites would be available at higher surface area of porous material. The S_{BET} was as high as 2025.9 $m^2\,g^{-1}$, indicating the suitability of activation procedure.

Surface morphologies of CM and AC-650-2 were evaluated using FESEM–EDX. During activation process, significant alterations occurred on the smooth, rigid and dense surface of CM. The EDX analysis showed that carbon and oxygen are the main elements of AC-650-2 (Supplementary Material). Moreover, the Na content of the AC was less than that of CM, indicating the efficient removal of NaOH residues in washing step. The chromium content of AC-650-2, after adsorption process, was as high as 10.3%, confirming the adsorption of a huge amount of chromium onto the adsorbent (Supplementary Material).

The presence of the pointed peaks in XRD pattern indicates crystalline nature of AC-650-2. The characteristic diffraction peaks at $2\theta = 10.20°$, 43.38°, 50.83° and 72.43° illustrate the carbon graphitic structure of AC-650-2 (Supplementary Material). After chromium adsorption at initial pH 2, the adsorbent lost some its crystallinity and became amorphous. This suggests that the chromium molecules diffused into the AC-650-2 pores and mainly chemisorbed on surface sites. Arulkumar et al. (2012) also reported the disappearance of the crystallinity of prawn shell-derived activated carbon after Cr(VI) adsorption.

3.4. Chemical surface characterization

FT-IR spectroscopy was used to identify the main characteristics functional groups present on the AC-650-2 surface, before and after chromium adsorption, and to determine the vibrational frequency changes. The FT-IR spectra of AC-650-2, before and after Cr(VI) adsorption, are shown in Supplementary Material. In fresh AC-650-2, the broad band observed at 3436 cm^{-1} indicates the presence of –OH group. The absorption peaks observed at 2923 and 2856 cm^{-1} correspond to the stretching vibration of C–H group. The band appeared at 1722 cm^{-1} is assigned to the carbonyl-stretching group (C=O). The peak at 1624 cm^{-1} can be attributed to the bending vibration of –NH group. The band at 1081 cm^{-1} is related with the C–O stretching vibration of phenolic, carboxylic, and alcoholic groups. After Cr(VI) adsorption, some changes were observed in the position and intensity of some peaks. The peaks related to –OH, C=O, –NH and C–O groups were changed to 3427, 1699, 1550 and 1099 cm^{-1}, respectively, while no change was observed in the position of C–H group related peaks. Therefore, the above changes in the FT-IR pattern may be attributed to

the interaction of Cr(VI) with the hydroxyl, carbonyl, amino and alkoxy groups present on the surface of AC-650-2.

Surface oxygen functional groups contribute significantly to adsorption process because they act as active sites capable of capturing adsorbate molecules (Pezoti et al., 2016). The method described by Boehm was used to quantify the functional groups present on the surface of AC-650-2. This method assumes that various surface oxygen groups with different acidities exist on sorbent surface, which can be neutralized by bases of different strengths (Martins et al., 2015). It was found that AC-650-2 has approximately $1.093\,mmol\,g^{-1}$ of acid groups and $0.73\,mmol\,g^{-1}$ of base groups on its surface. The acid groups are due to phenolic $(0.523\,mmol\,g^{-1})$ > lactonic $(0.492\,mmol\,g^{-1})$ > carboxylic $(0.078\,mmol\,g^{-1})$ groups.

The pH_{PZC} of a material refers to the pH value at which the net charge on the material surface is zero. The surface of material will be negatively charged at $pH > pH_{PZC}$ and positively charged at $pH < pH_{PZC}$ (Kumar and Jena, 2017b). The pH_{PZC} of AC-650-2 was found to be 7.0.

3.5. Effect of pH on Cr(VI) adsorption

As depicted in Fig. 2 (a), the pH of suspensions increased at the end of adsorption process at initial $pH < pH_{PZC}$ and vice versa. At $pH < pH_{PZC}$, hydrogen ion may be exhausted by reducing functional groups, while at $pH > pH_{PZC}$, the activated carbon neutralize alkali solution by release of H^+ of carboxyl and/or hydroxyl groups (Sun et al., 2014).

The RE of Cr(VI) was > 90% at $pH \leq 2$ (final $pH \leq 2.65$) and declined sharply to 35% at pH 3 (final $pH = 6.0$). With further increase in pH up to 9, the RE of Cr(VI) gradually decreased to 7% (Fig. 2a). These results indicated that the Cr(VI) sorption on AC-650-2 was strongly dependent on solution pH and was favored in acidic conditions.
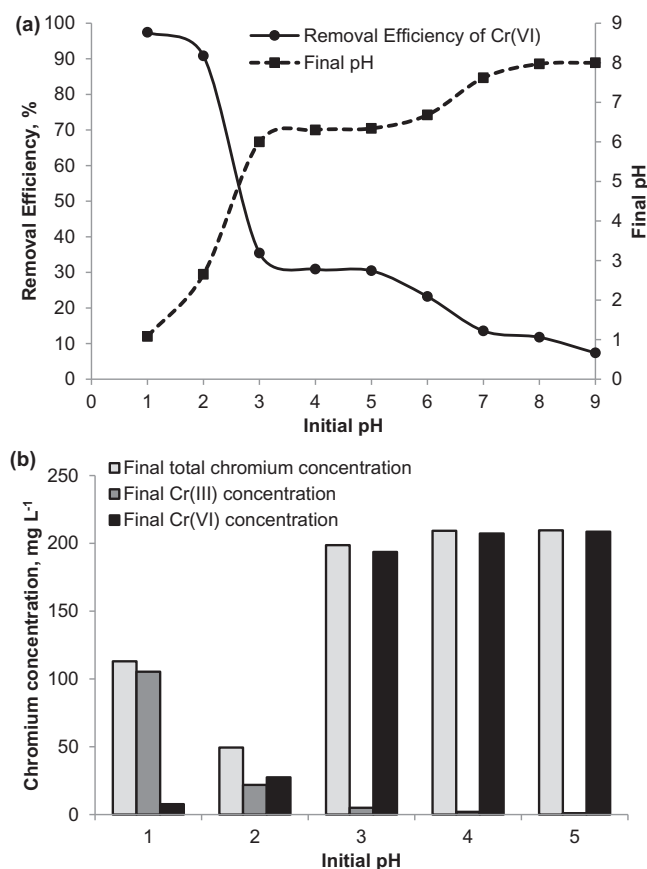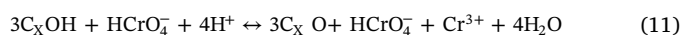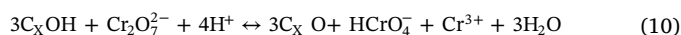

Fig. 2. (a) Cr(VI) removal efficiency and final pH as functions of initial pH and (b) chromium species concentrations at different pH levels.

Moreover, statistical analysis showed that the RE values were better correlated with the final pH values ($R^2 = 0.98$) than with the initial pH values ($R^2 = 0.79$). Therefore, the RE of Cr(VI) was mainly influenced by the final pH of the solutions. The preferred Cr(VI) adsorption in acidic conditions could be explained by considering both surface chemistry of the sorbent and chromium speciation in various pH values.

Hexavalent chromium may exist in the aqueous solution in several anionic forms depending on solution pH. CrO_4^{2-} is dominant at $pH > 6$, while $Cr_2O_7^{2-}$ and $HCrO_4^{1-}$ are the predominant Cr(VI) species at acidic pH (Gottipati and Mishra, 2016). At $pH < pH_{PZC}$, the surface charge of the AC-650-2 was positive, which favors the adsorption of Cr(VI) anions. With the decrease in solution pH, the extent of protonation on the surface of adsorbent would be increased, leading to a more strong attraction between Cr(VI) anions and sorbent surface. Moreover, the CrO_4^{2-} needs two active sites, whereas $HCrO_4^-$ only needs one active site and readily adsorbed on sorbent surface, resulting in higher sorption rate of Cr(VI).

Hexavalent chromium is a strong oxidizer due to its high positive redox potential ($E^0 \approx 1.3\,V$ at $pH \approx 1$ and $E^0 \approx 0.68\,V$ at $pH \approx 5$) (Sun et al., 2014). It may be reduced to Cr(III) in the presence of reducing functional groups on the AC-650-2 surface. Therefore, in pH effect experiments, the concentration of Cr(III) was also measured. In blank tests, the pH and initial chromium concentration remained unchanged and no Cr(III) was observed in the absence of AC, while some amount of Cr(III) was observed in the AC containing solutions. Therefore, a part of Cr(VI) was reduced to Cr(III) during redox reaction between reducing functional groups (C_xOH) and Cr(VI) according to the following reactions:

$$3C_XOH + Cr_2O_7^{2-} + 4H^+ \leftrightarrow 3C_X\,O + HCrO_4^- + Cr^{3+} + 3H_2O \qquad (10)$$

$$3C_XOH + HCrO_4^- + 4H^+ \leftrightarrow 3C_X\,O + HCrO_4^- + Cr^{3+} + 4H_2O \qquad (11)$$

where C_xO indicates the new oxygen containing functional groups resulted from Cr(VI) oxidation (Wang et al., 2009). Such redox reactions may cause some carbon loss (Zhang et al., 2017), which is reflected in EDX analysis of the AC, before and after chromium adsorption (Supplementary Material). As shown in Fig. 2(b), the concentration of Cr(III) at the end of adsorption process was higher at lower pH values. This phenomenon may be originated from the higher positive redox potential of Cr(VI) at more acidic conditions. Overall, the remained concentration of total chromium reached a minimum at initial pH 2.

3.6. Adsorption kinetics

Kinetic analysis of an adsorption system is important to understand the dynamics of adsorption in view of the order of the rate constants (Martins et al., 2015). The kinetics of Cr(VI)/AC-650-2 system were analyzed at initial pH values of 2 and 5. Fig. 3 shows the non-linear adjustments of the experimental data to the kinetic models. The magnitude of R^2 and RMSE values listed in Table 2 indicated that the adsorption of Cr(VI) onto the sorbent at both pH values was best fitted with Elovich kinetic model. Therefore, the adsorption of Cr(VI) onto AC-650-2 occurred predominantly by chemisorption. The Elovich model assumes that the sorbent surface is energetically heterogeneous and the kinetics of adsorption, at low surface coverage, is not influenced by desorption process or the interactions of adsorbate molecules (Pezoti et al., 2016). Very high values of α and very low values of β, especially at pH 2, indicating a low desorption rate due to an effective interaction between adsorbate and sorbent.

The experimental data of Cr(VI) adsorption onto AC-650-2 were also well fitted by Pseudo-second order model. This model suggests that the equilibrium amount of adsorbed adsorbate controls the number of binding sites (Gupta et al., 2011). Overall, as shown in Table 2, all the constants of Elovich and Pseudo-second order kinetic models imply that the adsorption of Cr(VI) onto AC-650-2 was more favorable at lower pH values.
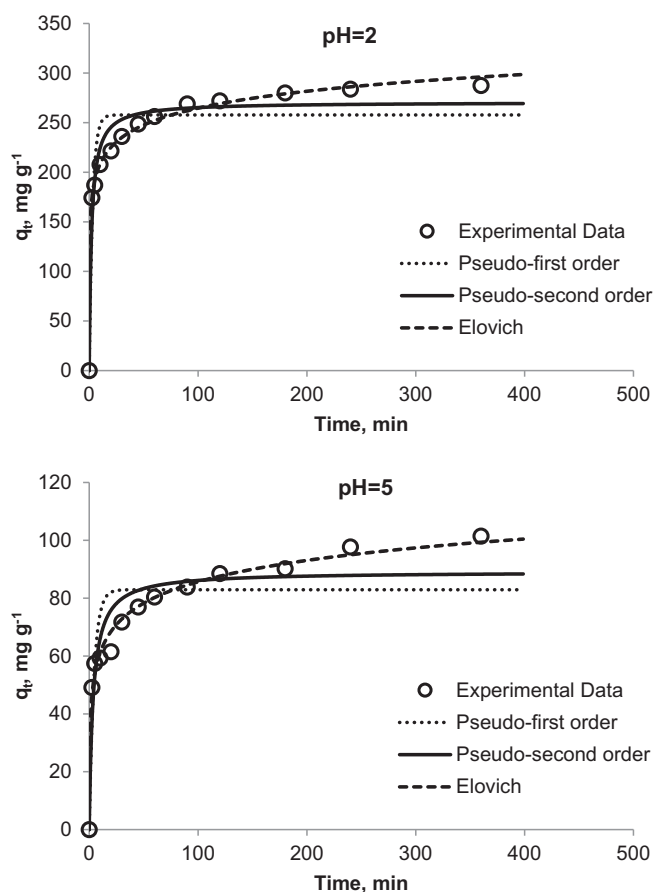
Fig. 3. Adsorption kinetic of Cr(VI) onto AC-650-2 and non-linear adjustments of the kinetic models (C$_0$ = 300 mg L^{-1}, T = 298 ± 0.5 K; 250 rpm for 2.5–360 min).

Table 2
Parameters of kinetic models for the adsorption of Cr(VI) onto AC-650-2.

	pH = 2	pH = 5
Pseudo-first order		
q$_e$ (mg g^{-1})	257.8	82.9
k$_1$ (min^{-1})	0.3207	0.2283
h$_0$ (mg g^{-1} min^{-1})	82.65	18.93
R^2	0.890	0.791
RMSE	24.44	11.68
Pseudo-second order		
q$_e$ (mg g^{-1})	270.7	89.2
k$_2$ (g mg^{-1} min^{-1})	0.0018	0.0032
h$_0$ (mg g^{-1} min^{-1})	131.14	25.36
R^2	0.958	0.895
RMSE	15.13	8.26
Elovich		
α (mg g^{-1} min^{-1})	11871.6	323.7
β (g mg^{-1})	0.04076	0.09360
R^2	0.997	0.988
RMSE	4.05	2.75

The Weber-Morris Intraparticle diffusion model was applied in order to understand how the diffusion of Cr(VI) molecules onto AC-650-2 takes place. This model assumes a multi-stages adsorption process including mass transfer of adsorbate molecules to the external surface of adsorbent, mass transfer of them to the internal surface of adsorbent, and their sorption onto the active sites of adsorbent (Coulibaly et al., 2016). The plots of q$_t$ versus (time)$^{0.5}$ for the adsorption of Cr(VI) onto AC-650-2 at pH values of 2 and 5 are presented in Supplementary Material. As can be seen, there are three stages of linearity for each adsorption condition. The first stage, starting from the origin, is related

Table 3
Parameters of Intraparticle diffusion for the adsorption of Cr(VI) onto AC-650-2.

Parameters	Initial solution pH	
	2	5
k$_{id,1}$ (mg g^{-1} min$^{-0.5}$)	88.56	26.69
C$_{i,1}$ (mg g^{-1})	7.75	1.56
k$_{id,2}$ (mg g^{-1} min$^{-0.5}$)	8.50	3.20
C$_{i,2}$ (mg g^{-1})	186.15	51.96
k$_{id,3}$ (mg g^{-1} min$^{-0.5}$)	1.33	1.08
C$_{i,3}$ (mg g^{-1})	262.44	81.03

to the transfer of Cr(VI) molecules from bulk liquid to the external surface of AC-650-2. The second stage is assigned to intraparticle diffusion, i.e. the entrance of Cr(VI) molecules into the porous structure of AC-650-2, while the third linear stage indicates the equilibrium phase (Coulibaly et al., 2016). The intercept value of the plots, C$_i$, characterizes the thickness of boundary layer. The C$_i$ values were in order of C$_1$ < C$_2$ < C$_3$ (Table 3), indicating the lower external diffusion resistance at the first stage of adsorption process, probably due to availability of more vacant adsorption sites.

The slope of the plots, k$_{id}$, characterizes the rate of adsorption process. As shown in Table 3, the value of k$_{id}$ for the first linear stage of adsorption at pH 2 (88.56 mg g^{-1} min$^{-0.5}$) was higher than that of pH 5 (26.69 mg g^{-1} min$^{-0.5}$). Therefore, in accordance to h$_0$ values of the Pseudo-second order model, the initial rate of Cr(VI) adsorption onto AC-650-2 was significantly higher in more acidic conditions.

Boyd's model was employed to identify if the rate-limiting step of adsorption is intraparticle diffusion or film diffusion. If the plot of B$_t$ versus time (Boyd's plot) be linear and passes through the origin, the intraparticle diffusion is the sole rate-limiting step in adsorption process; otherwise film diffusion governs the process (Cazetta et al., 2011). As shown in Supplementary Material, although the Boyd's plots present some linearity, they do not pass through the origin. Therefore, the film diffusion or chemical reaction controlled the adsorption rate of Cr(VI) onto AC-650-2 at both pH values.

3.7. Adsorption isotherm

Adsorption isotherms are used to understand how the adsorbate molecules are partitioned between the aqueous and solid phases under equilibrium condition (Martins et al., 2015). The equilibrium experimental data of Cr(VI) adsorption at pH values of 2 and 5 were analyzed by Langmuir, Freundlich, Redlich-Peterson and Temkin models and their non-linear fittings are shown in Fig. 4.

The Langmuir isotherm assumes that the adsorbate molecules form a monolayer on adsorbents with homogeneous surface, while Freundlich isotherm describes a multilayer adsorption onto heterogeneous surfaces (Nourmoradi et al., 2016). The Redlich-Peterson, a three-parameter model, is known as a compromise between Langmuir and Freundlich models (Pezoti et al., 2016). Temkin model promises that the heat of adsorption would change linearly, rather than logarithmic, with the coverage of adsorbent (Martins et al., 2015).

According to Table 4, Redlich-Peterson model better described the Cr(VI) adsorption at pH 2, while the Cr(VI) adsorption data at pH 5 were well fitted by Redlich-Peterson, Langmuir and Freundlich isotherm models. The Redlich-Peterson model admits both multi- and monolayer adsorption mechanisms. The exponent g in the model lies between 0 and 1. If g = 1, the Redlich-Peterson equation behaves as Henry's law. If g < 1 and the values of a$_{RP}$ and b$_{RP}$ parameters be far higher than 1, it converges to Freundlich approach. In the other hand, if g tends to ≈1, the Redlich-Peterson behaves according to Langmuir isotherm (Pezoti et al., 2016). As seen from Table 4, the g values were 0.95 and 0.75 for Cr(VI) adsorption at initial pH values of 2 and 5, respectively. The values of g, a$_{RP}$ and b$_{RP}$ parameters implies that the Cr
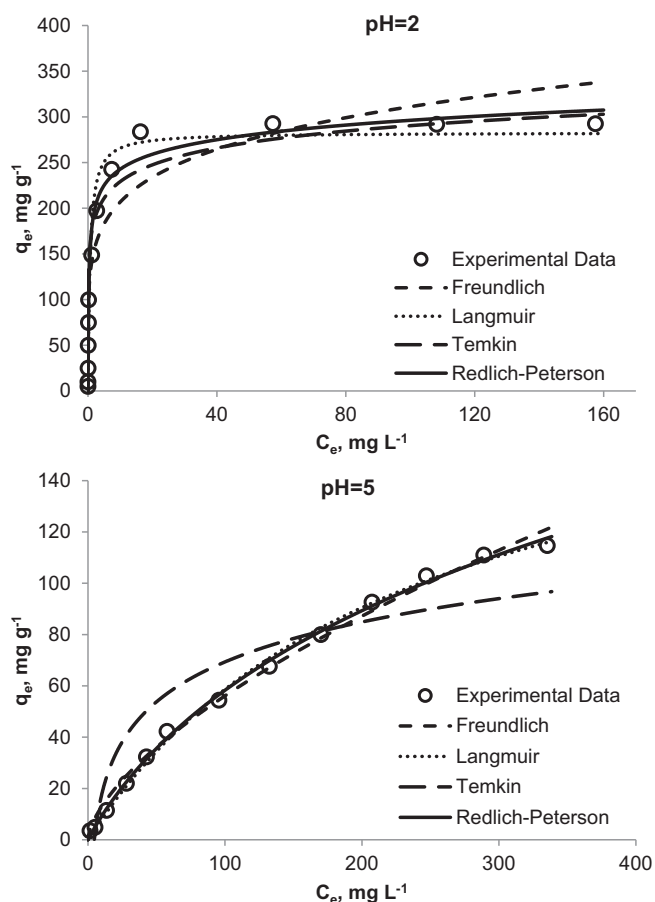
Fig. 4. Adsorption isotherm of Cr(VI) onto AC-650-2 and non-linear adjustments of the isotherm models ($C_0 = 5$–450 mg L^{-1}, T = 298 ± 0.5 K; 250 rpm for 240 min).

Table 4
Parameters of isotherm models for the adsorption of Cr(VI) onto AC-650-2.

	pH = 2	pH = 5
Freundlich		
k_F (mg g^{-1})	137.47	2.99
n_F	5.64	1.57
$1/n_F$	0.18	0.63
R^2	0.791	0.994
RMSE	33.00	2.96
Langmuir		
q_m (mg g^{-1})	282.8	198.0
k_L (L mg^{-1})	1.55	0.004
R^2	0.959	0.997
RMSE	21.77	2.13
Redlich-Peterson		
a_{RP} (L mg^{-1})$^{-g}$	965.03	1.05
b_{RP} (L g^{-1})	4.62	0.02
g	0.92	0.75
R^2	0.980	0.997
RMSE	14.44	1.85
Temkin		
k_T (L g^{-1})	529.35	0.219
b_T (J mol^{-1})	26.69	110.28
R^2	0.937	0.834
RMSE	27.04	15.27

(VI) adsorption at both pH values described by the Langmuir approach better than the Freundlich one. Therefore, the isotherm modeling suggests that the Cr(VI) adsorption onto AC-650-2 occurred in monolayers. An essential factor of the Langmuir isotherm is the separation factor (R_L), which can be used to verify if the adsorption process is favorable

Table 5
Comparison of maximum monolayer adsorption capacity (q_m) of Cr(VI) onto various biomass-derived activated carbons.

Precursor	Activating agent	pH	q_m (mg g^{-1})	Reference
Algal bloom residue	H_3PO_4	1	155.52	Zhang et al. (2010)
Tobacco residues	K_2CO_3	7	17.83	Kilic et al. (2011)
	KOH	8	0.55	
Peanut shell	KOH	4	13.28	Al-Othman et al. (2012)
Eichhornia crassipes root	H_2SO_4	4.5	36.34	Giri et al. (2012)
Sterculia guttata shell	$ZnCl_2$	2	90.90	Rangabhashiyam and Selvaraju (2015)
Longan seed	NaOH	2	169.49	Yang et al. (2015)
Bamboo bark	Steam	3	18.94	Zhang et al. (2015)
Bael fruit shell	$ZnCl_2$	2	43.54	Gottipati and Mishra (2016)
Mango kernel	H_3PO_4	2	7.80	Rai et al. (2016)
Fox nutshell	$ZnCl_2$	2	46.21	Kumar and Jena (2017a)
Fox nutshell	H_3PO_4	2	79.50	Kumar and Jena (2017b)
Date Press Cake	NaOH	2	282.80	Present study
		5	198.00	

($0 < R_L < 1$), linear ($R_L = 1$), or unfavorable ($R_L > 1$) (Martins et al., 2015). For the range of applied concentrations (5–450 mg L^{-1}), the R_L values decreased from 0.1140 to 0.0014 at pH 2 and from 0.9794 to 0.3455 at pH 5, indicating the favorability of Cr(VI) adsorption onto AC-650-2 in the concentration range studied. Overall, AC-650-2 showed the maximum monolayer adsorption capacities (q_m) of 282.8 and 198.0 mg g^{-1} at pH values of 2 and 5, respectively, which are excellent compared to the several biomass-derived ACs applied for Cr(VI) adsorption (Table 5).

3.8. Effect of ionic strength on Cr(VI) adsorption

The effect of ionic strength on Cr(VI) sorption was tested with deionized water containing various molar NaCl concentrations and real seawater at initial pH values of 2 and 5. As depicted in Fig. 5, the RE of Cr(VI) at initial pH 2 decreased from 94.6% to 75.2% as the NaCl concentration increased from 0 M to 1 M. The effect of ionic strength on Cr(VI) sorption was also tested with diluted and real seawater. Similarly, at pH 2, the rate of Cr(VI) adsorption in various seawater to deionized water (SW/DW) volume ratios showed a decreasing trend from 94.6% (deionized water) to 60.3% (real seawater). It has been demonstrated that the outer-sphere surface complexation is obviously
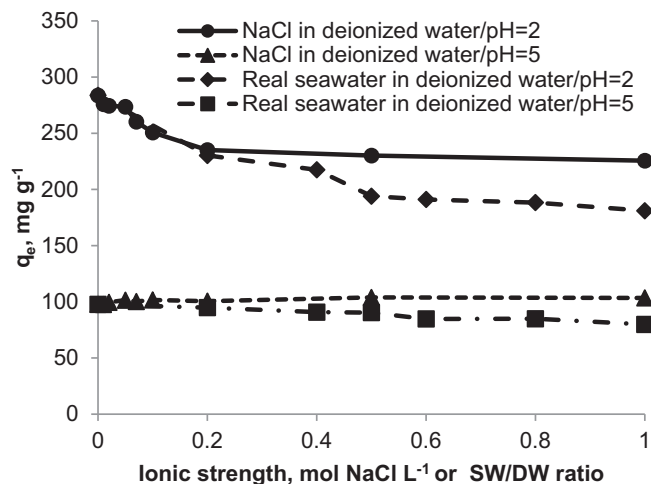

Fig. 5. Effect of ionic strength on Cr(VI) adsorption onto AC-650-2 ($C_0 = 300$ mg L^{-1}, T = 298 ± 0.5 K; 250 rpm for 240 min).

influenced by the changes in ionic strength of solution, while inner-sphere surface complexation is ionic strength independent (Fan et al., 2008). Therefore, electrostatic attraction (known as outer-sphere complexation) may play an important role in the adsorption of Cr(VI) onto AC-650-2 at initial pH 2. The decreased Cr(VI) adsorption rate at high ionic strengths could be attributed to the increase in the concentration of competitive anions and to the decrease in the ion activity of Cr(VI) ions.

As shown in Fig. 5, the ion strength originated from NaCl did not influence the Cr(VI) adsorption at initial pH 5. These results suggest that the sorption of Cr(VI) in near neutral conditions was ionic strength independent, indicating the negligible role of electrostatic attraction in the sorption system at these conditions. Alvarez-Ayuso et al. (2007) also reported that the dependency of Cr(VI) onto amorphous aluminum oxide was more pronounced in acidic conditions. The insensitivity to ionic strength is typical for the formation of inner-sphere complex, in which the adsorbed species and the sorbent surface establish covalent bonds (Goldberg, 2005). Note that, the negative effect of seawater on Cr(VI) adsorption at pH 5 may be due to the presence of organic matters. These compounds hamper the adsorption of metal ions through forming organic metal chelates and/or competing with them for surface adsorption sites (Liu et al., 2009).

3.9. Desorption studies

Disposal of AC-650-2 loaded with Cr(VI) can pose environmental issues because a portion of this hazardous metal may be leached out from the sorbent. Therefore, stripping Cr(VI) from the adsorbent may mitigate this problem to some extent. In this study, the desorption of Cr(VI) from AC-650-2 was initially evaluated with 0.1 M solutions of various eluents at 240 min contact time. The highest desorption rate was obtained by KOH (43.2%), followed in decreasing order by NaOH (41.6%), HNO_3 (2.6%), H_3PO_4 (2.5%), HCl (1.6%) and H_2SO_4 (0.7%). As discussed previously, Cr(VI) adsorption was favored in acidic condition and thus negligible desorption of Cr(VI) with acidic reagents was expectable. Subsequent tests were conducted with KOH and NaOH.

The desorption rates of Cr(VI) as a function of the concentration of desorbing solutions are presented in Supplementary Material. The desorption rate of Cr(VI) was increased with the increase in the concentration of KOH and NaOH solutions up to 0.5 M. The values were almost invariant with further increase in the concentration of the desorbing solutions.

The time variation for Cr(VI) desorption from AC-650-2 using 0.5 M desorbing solutions is shown in Supplementary Material. It is obvious that the initial rate of desorption was fast and the Cr(VI) desorption reached equilibrium during 120 min contact time. Overall, the desorption rates of 45.5% and 43.6% were obtained in 0.5 M KOH and NaOH solutions, respectively, at 120 min contact time.

All the above-mentioned desorption experiments were done with 0.025 g AC-650-2 in 25 ml solutions. By decreasing the volume of the desorbing solutions from 25 ml to 5 ml, the corresponding desorption rates decreased to 41.04% and 38.56%, respectively. Accordingly, the concentration of desorbed Cr(VI) in 5 ml of 0.5 M KOH and 0.5 M NaOH solutions increased by 4.51 and 4.42-fold, respectively. Concentrating the desorbed pollutant into the lower volumes of spent desorbing solutions may be economically and environmentally more favorable.

In accordance to some previous studies (Jing et al., 2011; Kumar and Tamilarasan, 2017), the desorption rate of Cr(VI) from the activated carbon prepared from DPC was not satisfactory. The incomplete desorption of Cr(VI) can be taken as an indication of irreversible chemisorption of Cr(VI) onto the sorbent (Giri et al., 2012).

3.10. Adsorption mechanism

The ionic states of the active functional groups of the adsorbent and chromium mainly depend on the pH of aqueous solution. Therefore, the pH of solution determined the predominant mechanism of Cr(VI) adsorption onto the surface of AC-650-2. Under acidic conditions, it seems that the electrostatic attraction had a significant role in the adsorption of Cr(VI) anions onto positively charged surface sites of the sorbent. This mechanism was more pronounced at pH < 3, at which monovalent species of Cr(VI) are readily adsorbed on the sorbent surface, resulting in higher adsorption rates. The effect of ionic strength on the adsorption system showed that the covalent bonds mainly established between Cr(VI) ions and the sorbent surface at near neutral conditions. The effect of solution pH also confirmed that a part of Cr(VI) was reduced to Cr(III) through contact with the electron donor sites presented on AC-650-2 surface. XRD analysis, adsorption isotherm modeling and desorption tests revealed that the Cr(VI) adsorption onto AC-650-2 was predominantly a chemisorption process. Moreover, Intraparticle diffusion and Boyd models indicated that the adsorption of Cr(VI) onto AC-650-2 was film diffusion controlled, confirming the chemisorption of Cr(VI) onto AC-650-2 surface.

4. Conclusion

The NaOH-activated carbon produced from Date Press Cake had high specific surface area and successfully adsorbed Cr(VI) anions from aqueous solution. The kinetic and isotherm experiments showed that the Cr(VI)/activated carbon system was best described by Elovich and Redlich-Peterson models. The prepared activated carbon showed maximum monolayer adsorption capacities as high as 282.8 and 198.0 mg g^{-1} at pH values of 2 and 5, respectively. Therefore, Date Press Cake could be considered as a potential precursor for the production of activated carbon, with a considerable potential for the adsorption of Cr(VI) from aqueous solutions.

Appendix A. Supplementary data

Supplementary data associated with this article can be found, in the online version, at https://doi.org/10.1016/j.biortech.2018.02.106.

References

Adinata, D., Daud, W.M.A.W., Aroua, M.K., 2007. Preparation and characterization of activated carbon from palm shell by chemical activation with K_2CO_3. Bioresour. Technol. 98 (15), 145–149.

Ahmaruzzaman, M., Gupta, V.K., 2011. Rice husk and its ash as low-cost adsorbents in water and wastewater treatment. Ind. Eng. Chem. Res. 50 (24), 13589–13613.

Al-Othman, Z.A., Ali, R., Naushad, M., 2012. Hexavalent chromium removal from aqueous medium by activated carbon prepared from peanut shell: adsorption kinetics, equilibrium and thermodynamic studies. Chem. Eng. J. 184, 238–247.

Alvarez-Ayuso, E., Garcia-Sanchez, A., Querol, X., 2007. Adsorption of Cr (VI) from synthetic solutions and electroplating wastewaters on amorphous aluminium oxide. J. Haz. Mater 142 (1), 191–198.

Arulkumar, M., Thirumalai, K., Sathishkumar, P., Palvannan, T., 2012. Rapid removal of chromium from aqueous solution using novel prawn shell activated carbon. Chem. Eng. J. 185, 178–186.

Basta, A.H., Fierro, V., El-Saied, H., Celzard, A., 2009. 2-Steps KOH activation of rice straw: an efficient method for preparing high-performance activated carbons. Bioresour. Technol. 100 (17), 3941–3947.

Cazetta, A.L., Vargas, A.M., Nogami, E.M., Kunita, M.H., Guilherme, M.R., Martins, A.C., Silva, T.L., Moraes, J.C., Almeida, V.C., 2011. NaOH-activated carbon of high surface area produced from coconut shell: kinetics and equilibrium studies from the methylene blue adsorption. Chem. Eng. J. 174 (1), 117–125.

Chandrasekaran, M., Bahkali, A.H., 2013. Valorization of date palm (Phoenix dactylifera) fruit processing by-products and wastes using bioprocess technology-review. Saudi J. Biol. Sci. 20 (2), 105–120.

Coulibaly, L.S., Akpo, S.K., Yvon, J., Coulibaly, L., 2016. Fourier transform infra-red (FTIR) spectroscopy investigation, dose effect, kinetics and adsorption capacity of phosphate from aqueous solution onto laterite and sandstone. J. Environ. Manage.

183, 1032–1040.

Fan, Q.H., Shao, D.D., Hu, J., Wu, W.S., Wang, X.K., 2008. Comparison of Ni^{2+} sorption to bare and ACT-graft attapulgites: effect of pH, temperature and foreign ions. Surf. Sci. 602 (3), 778–785.

FAO (Food and Agriculture Organization), 2014. FAOSTAT. Production; Crops. http://faostat3.fao.org/download/Q/QC/E (Accessed: 5 January 2018).

Fazlzadeh, M., Rahmani, K., Zarei, A., Abdoallahzadeh, H., Nasiri, F., Khosravi, R., 2017. A novel green synthesis of zero valent iron nanoparticles (NZVI) using three plant extracts and their efficient application for removal of Cr (VI) from aqueous solutions. Adv. Powder Technol. 28 (1), 122–130.

Federation, W.E., American Public Health Association, 2005. Standard Methods for the Examination of Water and Wastewater. American Public Health Association (APHA), Washington, DC, USA.

Foo, K.Y., Hameed, B.H., 2012. Potential of jackfruit peel as precursor for activated carbon prepared by microwave induced NaOH activation. Bioresour. Technol. 112, 143–150.

Ghnimi, S., Umer, S., Karim, A., Kamal-Eldin, A., 2017. Date fruit (Phoenix dactylifera L.): an underutilized food seeking industrial valorization. NFS J. 6, 1–10.

Giri, A.K., Patel, R., Mandal, S., 2012. Removal of Cr (VI) from aqueous solution by Eichhornia crassipes root biomass-derived activated carbon. Chem. Eng. J. 185, 71–81.

Goertzen, S.L., Thériault, K.D., Oickle, A.M., Tarasuk, A.C., Andreas, H.A., 2010. Standardization of the Boehm titration. Part I. CO_2 expulsion and endpoint determination. Carbon 48 (4), 1252–1261.

Goldberg, S., 2005. Inconsistency in the triple layer model description of ionic strength dependent boron adsorption. J. Colloid Interface Sci. 285 (2), 509–517.

Gottipati, R., Mishra, S., 2016. Preparation of microporous activated carbon from Aegle Marmelos fruit shell and its application in removal of chromium (VI) from aqueous phase. J. Ind. Eng. Chem. 36, 355–363.

Gupta, V.K., Agarwal, S., Saleh, T.A., 2011. Synthesis and characterization of alumina-coated carbon nanotubes and their application for lead removal. J. Hazard. Mater. 185 (1), 17–23.

Gupta, V.K., Saleh, T.A., 2013. Sorption of pollutants by porous carbon, carbon nanotubes and fullerene-an overview. Environ. Sci. Pollut. Res. 20 (5), 2828–2843.

Horikawa, T., Katoh, M., Tomida, T., 2008. Preparation and characterization of nitrogen-doped mesoporous titania with high specific surface area. Microporous Mesoporous Mater. 110 (2), 397–404.

Kilic, M., Apaydin-Varol, E., Pütün, A.E., 2011. Adsorptive removal of phenol from aqueous solutions on activated carbon prepared from tobacco residues: Equilibrium, kinetics and thermodynamics. J. Hazard. Mater. 189 (1), 397–403.

Kumar, A., Jena, H.M., 2017a. Adsorption of Cr (VI) from aqueous phase by high surface area activated carbon prepared by chemical activation with $ZnCl_2$. Process Saf. Environ. Prot. 109, 63–71.

Kumar, A., Jena, H.M., 2017b. Adsorption of Cr (VI) from aqueous solution by prepared high surface area activated carbon from Fox nutshell by chemical activation with H_3PO_4. J. Environ. Chem. Eng. 5 (2), 2032–2041.

Kumar, M., Tamilarasan, R., 2017. Kinetics, equilibrium data and modeling studies for the sorption of chromium by Prosopis juliflora bark carbon. Arab. J. Chem. 10, S1567–S1577.

Jing, G., Zhou, Z., Song, L., Dong, M., 2011. Ultrasound enhanced adsorption and desorption of chromium (VI) on activated carbon and polymeric resin. Desalination 279 (1), 423–427.

Liu, T., Rao, P., Mak, M.S., Wang, P., Lo, I.M., 2009. Removal of co-present chromate and arsenate by zero-valent iron in groundwater with humic acid and bicarbonate. Water Res. 43 (9), 2540–2548.

Liu, W.J., Zeng, F.X., Jiang, H., Zhang, X.S., 2011. Preparation of high adsorption capacity bio-chars from waste biomass. Bioresour. Technol. 102 (17), 8247–8252.

Martins, A.C., Pezoti, O., Cazetta, A.L., Bedin, K.C., Yamazaki, D.A., Bandoch, G.F., Asefa, T., Visentainer, J.V., Almeida, V.C., 2015. Removal of tetracycline by NaOH-activated carbon produced from macadamia nut shells: kinetic and equilibrium studies.

Chem. Eng. J. 260, 291–299.

Nourmoradi, H., Avazpour, M., Ghasemian, N., Heidari, M., Moradnejadi, K., Khodarahmi, F., Javaheri, M., Moghadam, F.M., 2016. Surfactant modified montmorillonite as a low cost adsorbent for 4-chlorophenol: equilibrium, kinetic and thermodynamic study. J. Taiwan Inst. Chem. Eng. 59, 244–251.

Owlad, M., Aroua, M.K., Daud, W.A.W., Baroutian, S., 2009. Removal of hexavalent chromium-contaminated water and wastewater: a review. Water Air Soil Pollut. 200 (1–4), 59–77.

Pawlisz, A.V., Kent, R.A., Schneider, U.A., Jefferson, C., 1997. Canadian water quality guidelines for chromium. Environ. Toxicol. 12 (2), 123–183.

Pehlivan, E., Altun, T., 2008. Biosorption of chromium (VI) ion from aqueous solutions using walnut, hazelnut and almond shell. J. Hazard. Mater. 155 (1), 378–384.

Pezoti, O., Cazetta, A.L., Bedin, K.C., Souza, L.S., Martins, A.C., Silva, T.L., Júnior, O.O.S., Visentainer, J.V., Almeida, V.C., 2016. NaOH-activated carbon of high surface area produced from guava seeds as a high-efficiency adsorbent for amoxicillin removal: kinetic, isotherm and thermodynamic studies. Chem. Eng. J. 288, 778–788.

Rai, M.K., Shahi, G., Meena, V., Meena, R., Chakraborty, S., Singh, R.S., Rai, B.N., 2016. Removal of hexavalent chromium Cr (VI) using activated carbon prepared from mango kernel activated with H_3PO_4. Resour.-Eff. Technol. 2, S63–S70.

Rangabhashiyam, S., Selvaraju, N., 2015. Adsorptive remediation of hexavalent chromium from synthetic wastewater by a natural and $ZnCl_2$ activated Sterculia guttata shell. J. Mol. Liq. 207, 39–49.

Sathishkumar, P., Arulkumar, M., Palvannan, T., 2012. Utilization of agro-industrial waste Jatropha curcas pods as an activated carbon for the adsorption of reactive dye Remazol Brilliant Blue R (RBBR). J. Clean. Prod. 22 (1), 67–75.

Silva, T.L., Cazetta, A.L., Souza, P.S., Zhang, T., Asefa, T., Almeida, V.C., 2017. Mesoporous activated carbon fibers synthesized from denim fabric waste: efficient adsorbents for removal of textile dye from aqueous solutions. J. Clean. Prod. 171, 482–490.

Sun, Y., Yue, Q., Mao, Y., Gao, B., Gao, Y., Huang, L., 2014. Enhanced adsorption of chromium onto activated carbon by microwave-assisted H_3PO_4 mixed with Fe/Al/Mn activation. J. Hazard. Mater. 265, 191–200.

Sun, J., Zhang, Z., Ji, J., Dou, M., Wang, F., 2017. Removal of Cr^{6+} from wastewater via adsorption with high-specific-surface-area nitrogen-doped hierarchical porous carbon derived from silkworm cocoon. Appl. Surf. Sci. 405, 372–379.

Tongpoothorn, W., Sriuttha, M., Homchan, P., Chanthai, S., Ruangviriyachai, C., 2011. Preparation of activated carbon derived from Jatropha curcas fruit shell by simple thermo-chemical activation and characterization of their physico-chemical properties. Chem. Eng. Res. Des. 89 (3), 335–340.

Wang, X.S., Li, Z.Z., Tao, S.R., 2009. Removal of chromium (VI) from aqueous solution using walnut hull. J. Environ. Manag. 90 (2), 721–729.

Wang, Y., Shu, L., Jegatheesan, V., Gao, B., 2010. Removal and adsorption of diuron through nanofiltration membrane: the effects of ionic environment and operating pressures. Sep. Purif. Technol. 74 (2), 236–241.

Xia, H., Cheng, S., Zhang, L., Peng, J., 2016. Utilization of walnut shell as a feedstock for preparing high surface area activated carbon by microwave induced activation: effect of activation agents. Green Process. Synth. 5 (1), 7–14.

Yang, J., Yu, M., Chen, W., 2015. Adsorption of hexavalent chromium from aqueous solution by activated carbon prepared from longan seed: kinetics, equilibrium and thermodynamics. J. Ind. Eng. Chem. 21, 414–422.

Zhang, H., Tang, Y., Cai, D., Liu, X., Wang, X., Huang, Q., Yu, Z., 2010. Hexavalent chromium removal from aqueous solution by algal bloom residue derived activated carbon: equilibrium and kinetic studies. J. Hazard. Mater. 181 (1), 801–808.

Zhang, Y.J., Ou, J.L., Duan, Z.K., Xing, Z.J., Wang, Y., 2015. Adsorption of Cr (VI) on bamboo bark-based activated carbon in the absence and presence of humic acid. Colloids Surf. A Physicochem. Eng. Asp. 481, 108–116.

Zhang, J., Chen, S., Zhang, H., Wang, X., 2017. Removal behaviors and mechanisms of hexavalent chromium from aqueous solution by cephalosporin residue and derived chars. Bioresour. Technol. 238, 484–491.